

[Article]

www.whxb.pku.edu.cn

新型二氟甲基磷酸类酪氨酸蛋白磷酸酯酶 1B 抑制剂的 分子动力学模拟和结合自由能计算

崔巍¹ 张怀² 计明娟^{1,*}¹中国科学院研究生院化学与化学工程学院, 北京 100049;²中国科学院研究生院计算地球动力学重点实验室, 北京 100049)

摘要: 通过分子对接建立了一系列含二氟甲基磷酸基团(DFMP)或二氟甲基硫酸基团(DFMS)的抑制剂与酪氨酸蛋白磷酸酯酶 1B(PTP1B)的相互作用模式, 并通过 1 ns 的分子动力学模拟和 molecular mechanics/generalized Born surface area (MM/GBSA)方法计算了其结合自由能. 计算获得的结合自由能排序和抑制剂与靶酶间结合能力排序一致; 通过基于主方程的自由能计算方法, 获得了抑制剂与靶酶残基间相互作用的信息, 这些信息显示 DFMP/DFMS 基团的负电荷中心与 PTP1B 的 221 位精氨酸正电荷中心之间的静电相互作用强弱决定了此类抑制剂的活性, 进一步的分析还显示位于 DFMP/DFMS 基团中的氟原子或其他具有适当原子半径的氢键供体原子会增进此类抑制剂与 PTP1B 活性位点的结合能力.

关键词: 酪氨酸蛋白磷酸酯酶 1B; 分子动力学模拟; 自由能计算; 自由能分解; MM/GBSA
中图分类号: O641

Molecular Dynamics Simulations and Free Energy Calculations of a Novel Series of Protein Tyrosine Phosphatase 1B Difluoromethylenephosphonic Acid Inhibitors

CUI Wei¹ ZHANG Huai² JI Ming-Juan^{1,*}¹College of Chemistry and Chemical Engineering, Graduate University of the Chinese Academy of Sciences, Beijing 100049, P. R. China; ²Laboratory of Computational Geodynamics, Graduate University of the Chinese Academy of Sciences, Beijing 100049, P. R. China)

Abstract: Binding models for a series of difluoromethylenephosphonic (DFMP) and difluoromethylenesulfonic (DFMS) acids to protein tyrosine phosphatase 1B (PTP1B) were studied by molecular docking, molecular dynamics (MD) simulations, and free energy calculations. Binding free energies were computed using the molecular mechanics/generalized Born surface area (MM/GBSA) methodology based on 1 ns MD simulations. The order of affinities for the studied inhibitors can be accurately predicted using previously predicted binding free energies. Inhibitor/residue interaction profiles for all inhibitors were systematically generated using MM/GBSA free energy decomposition analysis. Inhibitor/residue interaction profiles demonstrated that electrostatic interactions between the negative charge center of DFMP/DFMS groups and Arg221 of PTP1B are a crucial part of the studied molecule affinities. Furthermore, the fluorine atom or other hydrogen bonding donor atoms with appropriate radii will improve inhibitor binding to the primary binding site of PTP1B.

Key Words: Protein tyrosine phosphatase 1B; Molecular dynamics simulation; Free energy calculation; Free energy decomposition; MM/GBSA

Received: October 10, 2008; Revised: December 4, 2008; Published on Web: January 15, 2009.

*Corresponding author. Email: jmj@gucas.ac.cn; Tel: +8610-88256326; Fax: +8610-88256093.

国家自然科学基金(20373089)和中国科学院研究生院启动基金(M3004)资助项目

© Editorial office of *Acta Physico-Chimica Sinica*

Protein tyrosine phosphatases (PTPs) have been shown to play important roles in many biological processes governed by protein tyrosine phosphorylation^[1]. Protein tyrosine phosphatase 1B (PTP1B) is the first PTP isolated from homogeneous form and has been recognized as an important negatively regulator of insulin signaling by binding to and dephosphorylating insulin receptor tyrosine kinases^[2]. Recent studies with a PTP1B knock-out mouse result in insulin hypersensitivity^[3]. Thus, PTP1B is now recognized as a potential therapeutic target for treating type II diabetes and obesity^[3,4]. The active site region, which is targeted by many inhibitors, include residues on the PTP loop (Ser216, Ala217, Gly219, Gly220, and Arg221), the WPD loop (Asp181, Phe182), and the substrate recognition loop (Lys36, Val49, and Lys120). Some other inhibitors also interact with the secondary binding site of PTP1B, characterized by Tyr20, Arg24, His25, Phe52, and Arg254^[4].

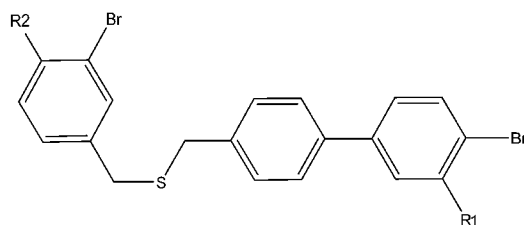
Since the phosphate group is crucial for PTP-substrate binding, the design of effective non-hydrolysable phosphate mimetics is an important research direction to find potential PTP1B inhibitors. The most effective phosphate mimetic reported to date is the difluoromethylenephosphonic acid (DFMP)^[5-12]. But, due to the dianionic nature of phosphonate groups in DFMP at physiological pH, the cell permeability and oral bioavailability of all DFMP inhibitors are very poor. On the other hand, because of the electrostatic properties of the enzyme active site^[13], it is very difficult to develop effective uncharged pTyr mimetics. Taylor and coworkers^[14] had constructed a hexapeptide bearing difluoromethylsulfonophenylalanine (F2Smp) peptide with a sequence of D-A-D-E-F2Smp-LNH2 and found that it was a better PTP1B inhibitor than analogous peptides bearing other monoanionic mimics. However, this peptide was still 100-fold less potent than the analogous peptide bearing the difluoromethylphosphonophenylalanine (F2Pmp) group (D-A-D-E-F2Pmp-LNH2)^[14]. Based on the DFMP inhibitors, Taylor and coworkers developed the PTP1B inhibitors with the difluoromethylenesulfonic acid (DFMS) group^[15], which is a monoanionic group and has less charge than the DFMP group at the physiological pH.

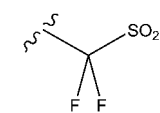
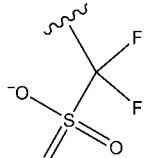
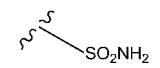
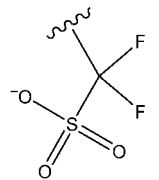
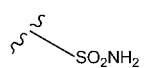
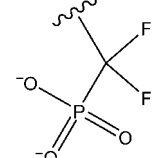
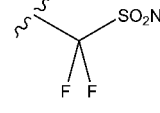
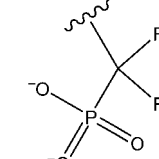
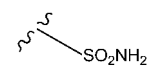
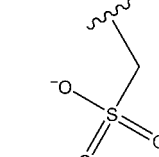
The inhibitors at the current work are shown in Table 1. The structures of those compounds are quite similar, but why they demonstrate different binding affinities with PTP1B. Meanwhile, why the non-peptide CF₂ sulfonates (compounds 1 and 2) are 1000-fold poorer inhibitors than their CF₂-phosphonate counterparts (compounds 3 and 4), and why the CF₂-phosphonate-bearing peptides are only 100-fold better inhibitors than the CF₂-sulfonate-bearing peptides^[14]? In order to answer these questions, molecular docking studies, MD simulations, and MM/GBSA free energy calculations^[16-22] were employed to build the binding models of all the compounds in the active site of the target enzyme and interpret the interactions between the compounds and PTP1B at the atomic level. The information obtained here will be helpful for finding better PTP1B inhibitors.

1 Materials and methods

1.1 Structures of PTP1B and inhibitors

Table 1 Structures and *in vitro* activity of DFMS & DFMP PTP1B inhibitors



Compound	R1	R2	IC ₅₀ (μmol·L ⁻¹) ^[15]
1			6
2			10
3			0.006
4			0.030
5			21

The crystal structure of PTP1B was obtained from the Brookhaven protein data bank (PDB entry: 1KAV)^[23]. The ligand in 1kav is similar to the five compounds studied here. The crystallographic waters and the ligand were artificially removed from 1KAV.

The five inhibitors were built in SYBYL 7.1^[24]. Then all of the inhibitors were minimized by the Hartree-Fock/6-31G* optimization in Gaussian 03^[25], and the atom partial charges were obtained by fitting the electrostatic potentials derived by Gaussian 03^[25] using the RESP technique^[26] in AMBER 9^[27]. The generation of the partial charges and the force field parameters for the inhibitors was accomplished using the antechamber program in AMBER 9^[27].

1.2 Molecular docking simulation

In order to tackle the binding modes of the inhibitors in the

active site of PTP1B, the AutoDock program^[28] was used to simulate the molecular docking. The Lamarckian genetic algorithm (LGA)^[28] was applied to optimize the binding conformations of inhibitors in the active site. AutoDock can only deal with atom types less than 6. According to the structure and atom types of all those 5 compounds, we used compound 5 and compound 1 (all fluorine atoms were changed to hydrogen atoms) as templates to perform the docking studies. The docking calculation was performed in a three dimensional grid with $100 \times 100 \times 100$ points and a spacing of 0.0375 nm, located in both the primary binding site and the secondary binding site. There are 256 runs of LGA optimization for each compound. For each run the numbers of generations and the energy evaluations were set to 90000 and 1500000, respectively. After 256 runs of docking calculation 256 conformations were generated, and then they were clustered by root mean squared deviations (RMSDs) of these conformations. The most popular cluster was selected as the binding cluster.

Compound 1 in the predicted complex was modified to compound 2, and compound 5 in the predicted complex was modified to compounds 3 and 4 by changing the atom types. Then all the predicted complexes were minimized using the MMFF94 force field in SYBYL 7.1^[24].

1.3 Molecular dynamics simulation

MD simulations were carried out in AMBER 9 for the predicted complexes generated by AutoDock^[27]. In the following MD simulations, AMBER03 (parm03) force field^[29] was used to establish the potentials of proteins, and general amber force field (gaff)^[30] was used to establish the potentials of inhibitors. The missing hydrogen atoms of protein were added using the tleap program in AMBER 9. To neutralize the charge of the systems, Na⁺ ions were placed to the grids with the strongest negative Coulombic potentials around PTP1B, and then the whole system was immersed in the rectangular truncated octahedron of TIP3P water molecules^[31]. The water box extended 1.2 nm away from any solute atoms.

Prior to MD simulations, the complex structures were minimized in three steps. First, all non-solute atoms were fixed and the water molecules were optimized (2000 cycles of steepest descent and 2000 cycles of conjugate gradient minimizations); then, all backbone atoms were fixed, and the side-chains, ligand, and solvent were optimized (2500 cycles of steepest descent and 2500 cycles of conjugate gradient minimizations); finally, the whole system was optimized (2500 cycles of steepest descent and 2500 cycles of conjugate gradient minimizations) without any constrain.

The system was gradually heated in the canonical ensemble from 0 to 310 K over 60 ps. Then 1 ns MD simulation was performed under constant temperature of 310 K as body temperature by the weak-coupling algorithm^[32]. During the MD simulations, SHAKE^[33] was used to fix all bonds involving hydrogen atoms and the time step was set to 2 fs. Particle mesh Ewald (PME)^[34] was employed to deal with the long-range electrostatic

interactions. During the sampling process coordinates were saved every 0.2 ps.

1.4 MM/GBSA calculation and MM/GBSA free energy decomposition analysis

MM/GBSA procedure was performed to calculate the binding free energy of the studied inhibitors according to the following equation^[35,36]:

$$\Delta G_{\text{binding}} = G_{\text{complex}} - G_{\text{protein}} - G_{\text{ligand}} \\ = \Delta E_{\text{MM}} + \Delta G_{\text{GB}} + \Delta G_{\text{SA}} - T\Delta S \quad (1)$$

where G_{binding} means the binding free energy of the binding process, G_{complex} , G_{protein} , and G_{ligand} are the free energies of protein-ligand complex, protein, and ligand, respectively. ΔE_{MM} is the molecular mechanics interaction energy between the protein and the inhibitor, ΔG_{GB} and ΔG_{SA} are the electrostatic and non-polar contributions to desolvation upon inhibitor binding, respectively, and $-T\Delta S$ is the change of conformational entropy^[16].

The polar solvation free energy was calculated by the generalized Born (GB) approximation model developed by Tsui *et al.*^[37]. In the GB calculations, the solvent and solute dielectric constants are set to 80 and 4, respectively. The non-polar solvation term was estimated for the surface area. The protein-ligand binding free energy was calculated for the 120 snapshots extracted from the MD trajectory from 0.4 to 1.0 ns. The conformation entropy was not considered here because of its high computational demand and relatively low accuracy of predictions^[17].

The PTP1B/inhibitor interaction profiles were generated from decomposing the total binding free energies into residue/inhibitor interaction pairs by the MM/GBSA decomposition process in the mm_pbsa program of AMBER 9^[38,39]. The binding interaction of each inhibitor-residue pair includes three terms: van der Waals contribution (ΔE_{vdw}), electrostatic contribution (ΔE_{ele}), and solvation contribution ($\Delta G_{\text{GB}} + \Delta G_{\text{SA}}$),

$$\Delta G_{\text{inhibitor-residue}} = \Delta E_{\text{vdw}} + \Delta E_{\text{ele}} + \Delta G_{\text{GB}} + \Delta G_{\text{SA}} \quad (2)$$

where ΔE_{vdw} and ΔE_{ele} are non-bonded van der Waals interaction and electrostatic interaction between inhibitor and each protein residue, which can be computed using the sander program in AMBER 9^[27]. The polar contribution (ΔG_{GB}) of desolvation was computed with the GB model, and the nonpolar contribution of desolvation (ΔG_{SA}) was computed as the surface area. The charges used in GB calculations were taken from the AMBER parameter set^[38,39]. The snapshots generated for MM/GBSA calculation were used in energy decomposition calculation.

2 Results and discussion

2.1 Binding models predicted by molecular docking studies

The predicted binding models for all the five inhibitors are shown in Fig.1. All the conformations are the averaged structures for all snapshots extracted from the MD simulation trajectories. The binding models of the five compounds are quite similar: the CF₂-phosphonate/sulfonate groups bind to the primary active site, including residues Tyr46, Asp48, Val49, Cys215, Ser216, Ala217, Gly218, Ile219, Gly220, and Arg221, and the

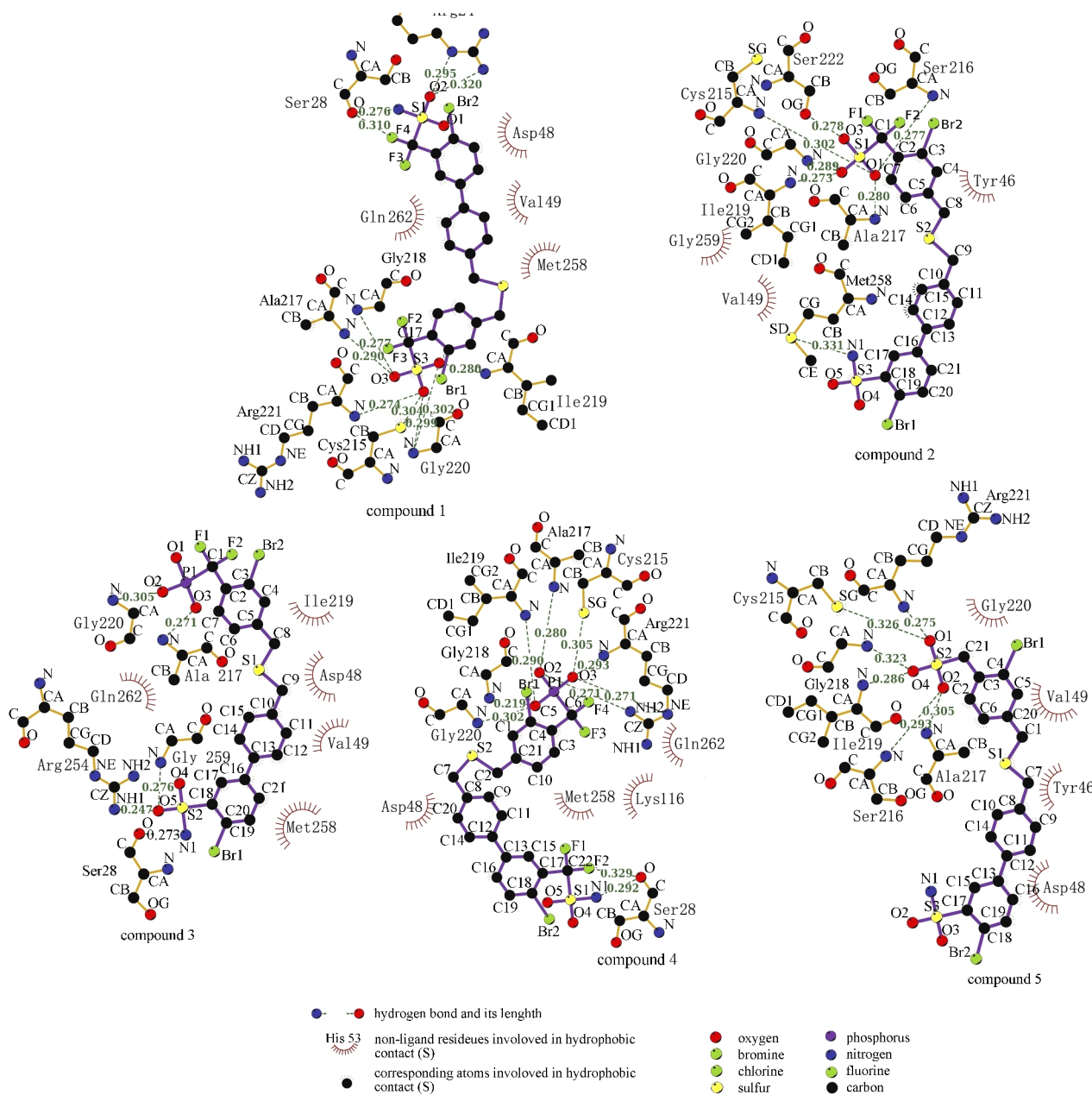


Fig.1 Schematic representation of interactions between inhibitors and PTP1B predicted by molecular docking studies

This figure was produced by the Ligplot program developed by Wallace *et al.*^[60].

sulfuryamide groups are located in the secondary active site, including Arg24, Ser28, Arg254, Met258, Gly259, and Gln 262.

2.2 Molecular dynamics simulation

The time evolutions of potential energies and RMSDs over the lowest conformation in MD simulation trajectories for all the five inhibitor/PTP1B complexes are shown in Fig.2. The potential energies show that all five complexes are stable after about 100 ps. The RMSD plots show that the value reaches the lowest point at about 400 ps, which indicates that the conformations of the complexes usually achieve equilibrium after 400 ps.

Detailed analyses of root-mean-square fluctuation (RMSF) of backbone atoms *versus* the residue number for five complexes and a single PTP1B are illustrated in Fig.3. Overall the distribu-

tions of RMSF for the six structures are quite similar. The RMSF values of these residues located at the active sites are obviously lower than other residues, which implies that the residues located at the active site are relatively stable. The average RMSF values of all the residues interactive with the five complexes (including active site residues and secondary site residues) are 0.2518, 0.2450, 0.2289, 0.3516, and 0.3044 nm, respectively, and the same value of a single PTP1B is 0.3722 nm. The average RMSF values of the residues in the primary active site of the five complexes and signal PTP1B are 0.2437, 0.2487, 0.2109, 0.3521, 0.3022, and 0.3896 nm, respectively; and those of the residues in the secondary site are 0.2628, 0.2417, 0.2536, 0.3512, 0.3064, and 0.3373 nm, respectively. The average RMSF values

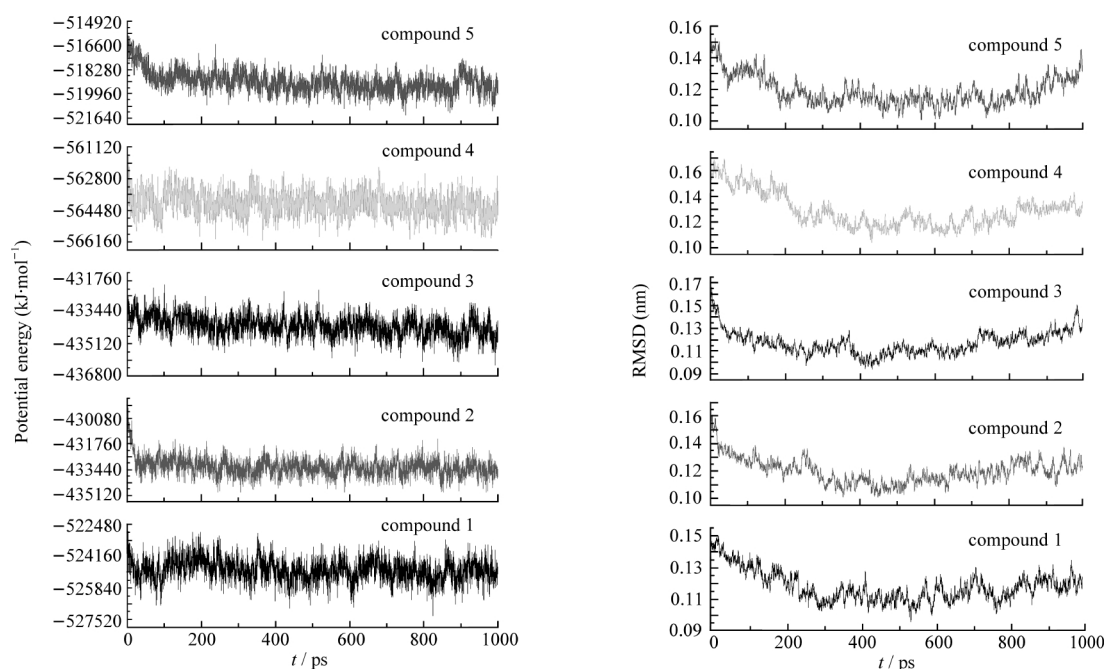


Fig.2 Evolution of the potential energies and the root-mean-square deviations (RMSD) compared with the structures minimized from the lowest conformation in MD simulation trajectories as a function of time

The RMSD values were calculated for all solute atoms against the lowest structure during the whole MD simulations.

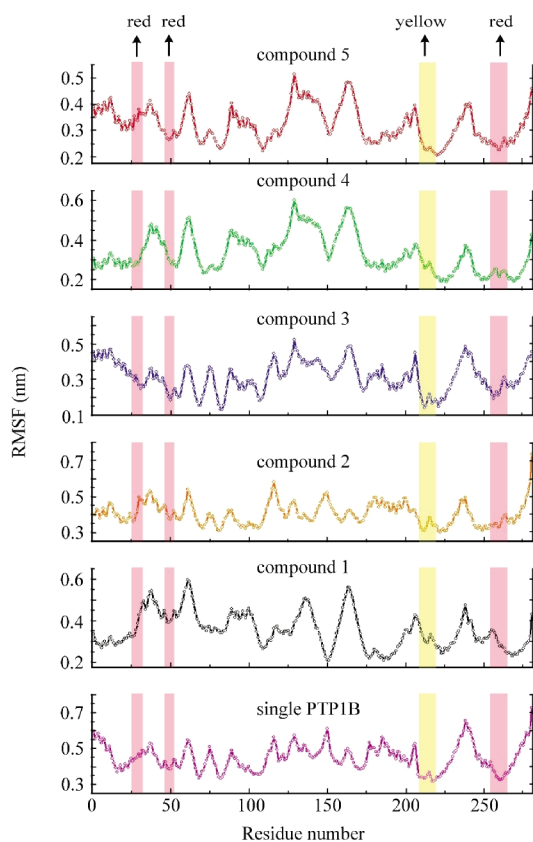


Fig.3 Root-mean-square fluctuation (RMSF) of backbone atoms versus residue number of the five complexes

Residues located in active site are marked by yellow background; residues located in second binding site are marked by red background.

of all residues of the five complexes and single PTP1B are 0.3215, 0.3308, 0.3136, 0.4033, 0.3520, and 0.4487 nm, respectively. For all five compounds the average RMSF values of binding site residues are about 70%–80% of those in all residues. The average RMSF of active site and secondary binding site residues in five complexes are much lower than the same value in single PTP1B.

2.3 MM/GBSA free energy calculation

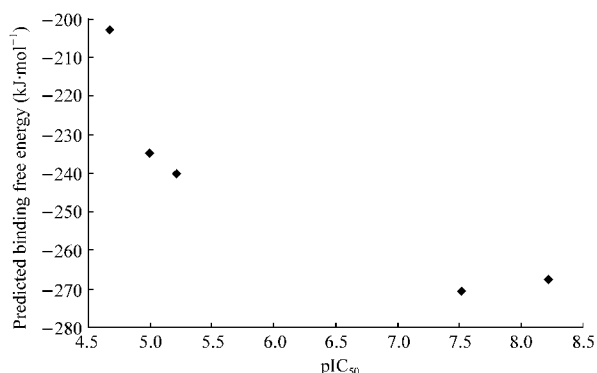
The results of the MM/GBSA calculation and the experimental binding data are shown in Table 2. The correlation coefficient (r) of the predicted binding energies and the experimental data (pIC_{50}) is 0.892 shown in Fig.4. The calculation results show that the CF_2 -phosphonate compounds have about $20 \text{ kJ} \cdot \text{mol}^{-1}$ more favorable interactions with PTP1B than the CF_2 -sulfonate compounds. We compared the correlations between the difference $\Delta\Delta G_{\text{tot}}$ between ΔG_{tot} of compounds with DFMP group and DFMS group and each of the four energy components. For $\Delta\Delta G_{\text{vdw}}$, $\Delta\Delta G_{\text{ele}}$, $\Delta\Delta G_{\text{GB}}$ and $\Delta\Delta G_{\text{SA}}$, the correlation coefficients are -0.391 , 0.907 , -0.848 , and 0.312 , respectively, suggesting that the difference of the electrostatic interactions can be used to distinguish the bindings between the CF_2 -phosphonate compounds and the CF_2 -sulfonate compounds.

2.4 MM/GBSA energy decomposition analysis

In order to gain a clear picture about the contribution of each PTP1B residue to binding, the total binding free energy was decomposed into residue/inhibitor interaction pairs using the MM/GBSA energy decomposition analysis (Table 3). The quantitative information is extremely useful to understand the binding mechanism of the PTP1B inhibitors. According to analysis, we can find that seven residues (print in bold type in Table 3) locat-

Table 2 Binding free energies and the individual energy components (in kJ·mol⁻¹)

Compound	ΔG_{ele}	ΔG_{vdw}	ΔG_{SA}	ΔG_{GB}	ΔG_{tot}	$\text{IC}_{50}(\mu\text{mol}\cdot\text{L}^{-1})^{[15]}$
1	-198.66±2.52	-199.08±5.88	-27.30±0.42	185.22±3.36	-240.24±5.46	6
2	-234.78±4.62	-180.60±15.12	-23.94±1.26	204.54±4.20	-234.78±17.22	10
3	-510.30±17.64	-179.34±4.62	-25.62±0.84	447.72±15.54	-267.54±7.98	0.006
4	-501.06±15.96	-181.86±7.98	-28.98±0.42	443.94±12.60	-270.48±6.72	0.030
5	-203.28±6.72	-162.96±14.28	-23.10±2.10	163.80±5.46	-202.86±17.64	21

**Fig.4 Predicted binding free energy versus pIC₅₀ of the five complexes**

ed in the primary binding site have significant contributions (>4.2 kJ·mol⁻¹). Among the seven residues, Arg221 is the most important one. According to energy decomposition analysis, Arg221 always forms very strong interaction with all inhibitors, especially with compounds 3 and 4. All four energy terms of interactions

Table 3 Interactions (in kJ·mol⁻¹) between the inhibitors and the important residues of PTP1B based on the MM/GBSA energy decomposition analysis

Residue	No.	Compound				
		1	2	3	4	5
Arg	24	-6.0984	-1.5792	-1.7976	-6.4512	-0.9576
Ala	27	-1.1760	-0.1848	-4.0740	-0.4200	-0.3780
Ser	28	-2.6628	-0.3192	-5.5776	-3.9648	-0.2016
Asp	29	-3.1416	-0.8064	0.0504	-1.5792	-0.1008
Tyr	46	-4.7964	-4.4016	-4.2420	-5.5608	-6.4176
Asp	48	-4.6032	-5.4852	-3.1752	-3.1584	-6.6444
Val	49	-6.0648	-7.4004	-7.3332	-6.3588	-7.8876
Phe	52	-0.9324	-0.8484	-1.4700	-0.2268	-0.8652
Cys	215	-4.6452	-6.3504	-7.0224	-10.1304	-5.1240
Ser	216	-4.7628	-6.0396	-11.4156	-8.3832	-6.3672
Ala	217	-11.1048	-12.0792	-14.5908	-15.2124	-11.5164
Gly	218	-5.4432	-5.1072	-8.0136	-8.1228	-5.2836
Ile	219	-11.8608	-9.6096	-14.9520	-15.2040	-10.4076
Gly	220	-6.0144	-4.0740	-8.5260	-9.5676	-5.7456
Arg	221	-11.6844	-9.8952	-30.3996	-30.7524	-11.1636
Arg	254	-2.5368	-1.9236	-2.7552	-2.8812	-0.9324
Met	258	-8.3244	-8.9292	-11.6844	-6.0396	-6.9048
Gly	259	-2.8056	-3.3180	-3.9480	-2.5536	-1.3104
Leu	260	-0.8820	-0.7392	-1.176	-1.2432	-0.6300
Gln	262	-8.0052	-5.5272	-6.7284	-11.4744	-5.0736
Gln	266	-2.3604	-0.7056	-2.0412	-3.4272	-0.7896

between Arg221 and the compounds are shown in Table 4. The guanidine group of Arg221 can form strong electrostatic interactions with the terminal oxygen atoms of the inhibitors, especially for the CF₂-phosphonate compounds, such as compound 3 (-97.4652 kJ·mol⁻¹) and compound 4 (-97.4820 kJ·mol⁻¹). On the other hand, the desolvation of CF₂-phosphonate compounds with Arg221 is quite unfavorable, which is 68.5272 kJ·mol⁻¹ for compound 3 and 66.0240 kJ·mol⁻¹ for compound 4. If we consider ΔG_{ele} and ΔG_{GB} together, the interactions between Arg221 and the terminal oxygen of inhibitors are still very favorable, especially for the CF₂-phosphonate compounds.

To investigate which energy component of interactions between the PTP1B residues and inhibitors determines the difference of the affinities between CF₂-phosphonate compounds and CF₂-sulfonate compounds, we calculated the difference of each inhibitor-residues interaction energy term between compound 2 and compound 3 (Table 5). It can be observed that among those seven residues located in the primary active site, Arg221 is not only the most important one for binding, but also for distinguishing the affinities of the CF₂-phosphonate inhibitors and those of the CF₂-sulfonate inhibitors.

Furthermore, the individual energy components contributed by the PTP1B residues located at binding site were correlated with the total binding free energies of those residues. For the CF₂-sulfonate compounds, the correlation coefficients of ΔG_{vdw} , ΔG_{ele} , ΔG_{GB} , and ΔG_{SA} with the ΔG values of the PTP1B residues are 0.920, 0.353, -0.277, and 0.545, respectively. For the CF₂-phosphonate compounds the corresponding values are 0.222, 0.772, -0.681, and 0.220, respectively. For these four energy terms, ΔG_{vdw} has the best correlation with ΔG for the less charged systems (CF₂-sulfonate compounds) and ΔG_{ele} has the best correlation with ΔG for more charged systems (CF₂-phosphonate compounds). Therefore, for the less charged molecules, the van der Waals interactions determine the binding preference, while for the more charged molecules, the electrostatic interactions determine the binding preference.

Table 4 Interactions (in kJ·mol⁻¹) between the inhibitors and Arg221 of PTP1B based on the MM/GBSA energy decomposition analysis

Compound	ΔG_{ele}	ΔG_{vdw}	ΔG_{SA}	ΔG_{GB}	ΔG
1	-34.5072	-5.7288	29.1984	-0.6468	-11.6844
2	-28.6272	-6.3840	25.6032	-0.4788	-9.8952
3	-97.4652	-0.8904	68.5272	-0.5628	-30.3996
4	-97.4820	1.1340	66.0240	-0.4284	-30.7524
5	-32.9868	-4.1748	26.5524	-0.5544	-11.1636

Table 5 Difference between compound 2/residue interactions and compound 3/residue interactions based on the MM/GBSA energy decomposition analysis (in $\text{kJ}\cdot\text{mol}^{-1}$)

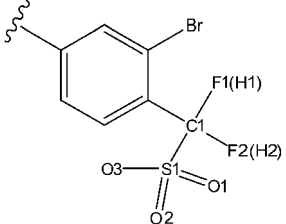
Residue	No.	$\Delta\Delta G_{\text{vdw}}$	$\Delta\Delta G_{\text{ele}}$	$\Delta\Delta G_{\text{GB}}$	$\Delta\Delta G_{\text{SA}}$	$\Delta\Delta G$
Arg	24	-0.2688	11.9196	-11.3064	-0.1344	0.2184
Ala	27	2.7972	1.5456	-1.0500	0.5796	3.8892
Ser	28	3.0660	3.1752	-1.5960	0.6300	5.2584
Asp	29	-0.4368	-6.5436	6.5184	-0.3948	-0.8568
Tyr	46	0.1428	-0.2520	0.0252	-0.1008	-0.1596
Asp	48	-1.3524	-15.0780	14.3136	-0.2100	-2.3100
Val	49	-0.2688	0.2184	0.0504	-0.0588	-0.0672
Phe	52	0.6384	-0.0168	0.0000	-0.0084	0.6216
Cys	215	-4.1160	8.9040	-3.6876	-0.4284	0.6720
Ser	216	-0.4536	10.4748	-4.6284	-0.0168	5.3760
Ala	217	-1.6968	5.5524	-1.2180	-0.1008	2.5116
Gly	218	-0.7140	3.5196	0.1596	-0.0084	2.9064
Ile	219	1.1004	5.2080	-0.9324	-0.0336	5.3424
Gly	220	-0.6384	7.2828	-2.1504	-0.0588	4.4520
Arg	221	-5.4936	68.8380	-42.9240	0.0840	20.5044
Arg	254	0.1344	12.0540	-11.3736	0.0084	0.8316
Met	258	2.9064	-0.7476	0.5124	0.0504	2.7552
Gly	259	0.5880	-0.9912	0.9408	0.1092	0.6300
Leu	260	0.1260	0.8064	-0.4788	0.0000	0.4368
Gln	262	0.4368	2.0160	-1.2852	0.0252	1.2012
Gln	266	0.7644	2.4612	-2.1084	0.2100	1.3356

2.5 Atom partial charges of compound 2 and compound 5

Compound 2 and compound 5 were selected as samples to understand the function of fluorine atoms in DFMS group. We compared the atom partial charges of R2 group of the two compounds (Table 6).

According to Table 6 there are less negative charges distributed in sulfonic acid groups of compound 2 than that in compound 5. This fact prompts that the methylenesulfonic acid with fluoro atoms is easy to loss its proton, which may reduce the electronic interactions between DFMS group and Arg221. On the other hand, the fluorine atoms in compound 2 with negative charge

Table 6 Atom partial charges (e) of DF(H)MS group in compound 2 and compound 5



	C1	F1(H1)	F2(H2)	S1	O1/O2/O3	Total charge
Compound 2	0.2852	-0.1979	-0.1979	1.0789	-0.6459	-0.9694
Compound 5	-0.8116	0.2282	0.2282	1.3541	-0.7256	-1.1779

may become hydrogen bond donors, which is helpful for DFMS groups to form stable interactions with active site of PTP1B.

2.6 Hydrogen bond analysis

To investigate the difference between compound 2 and compound 5, we analyze the hydrogen bond interactions between the CF_2 -sulfonate groups of inhibitors and PTP1B during the whole MD trajectory (Table 7). We also analyze the details of hydrogen bonds between R2 group of inhibitors and the active site of PTP1B (Fig. 5). In the averaged snapshot of the MD trajectory, there are 3.34 hydrogen bonds formed between compound 2 and PTP1B and only 2.39 hydrogen bonds formed between compound 5 and PTP1B.

According to Table 7, the hydrogen bonds between compound 2 and PTP1B are more stable than those between compound 5 and PTP1B. It should be noted that a hydrogen bond involving the fluorine atom in the CF_2 -sulfonate group can be found in 52.91% of snapshots from the MD simulations. This hydrogen bond is essential to lock the backbone N atom of Arg221, which is the most important residue for electrostatic interaction between inhibitor and PTP1B. Due to this hydrogen bond the CF_2 -sulfonate group forms more stable interactions with the primary active site of PTP1B than with the CH_2 -sulfonate group.

Burke *et al.*^[41] had reported that the high affinity of DFMP

Table 7 Hydrogen bonds between compound 2/5 with the residues in the primary active site

Compound	Donor	Acceptor	Occupied ^a	Distance (nm) ^b	Angle ($^\circ$) ^c	Life time (ps)
2	O2@inhibitor	H@ILE219-N@ILE219	97.43	0.279±0.008	17.78±8.72	38.6
	O2@inhibitor	H@GLY220-N@GLY220	87.96	0.285±0.008	16.50±9.70	8.7
	O1@inhibitor	H@SER216-N@SER216	82.51	0.285±0.008	16.01±9.45	5.3
	O1@inhibitor	H@ALA217-N@ALA217	81.35	0.285±0.008	26.42±12.81	5.3
	F1@inhibitor	H@ARG221-N@ARG221	52.91	0.288±0.008	26.33±11.42	2.1
	O1@inhibitor	H@GLY218-N@GLY218	18.02	0.293±0.005	15.68±8.77	1.2
	O2@inhibitor	H@GLY218-N@GLY218	12.36	0.291±0.006	50.25±7.36	1.2
	5	O4@inhibitor	H@GLY220-N@GLY220	82.72	0.285±0.008	16.38±9.33
O4@inhibitor		H@ILE219-N@ILE219	80.70	0.284±0.009	22.10±8.86	5.4
O1@inhibitor		H@ARG221-N@ARG221	73.10	0.286±0.008	22.49±10.90	4.0
O5@inhibitor		H@ALA217-N@ALA217	66.68	0.286±0.008	17.32±10.21	3.2
O1@inhibitor		HG@CYS215-SG@CYS215	13.34	0.295±0.004	34.98±13.05	1.3

a) percentage of snapshots in which the H-bond formed during MD simulation; b) average values and standard errors of the H-bond distance in MD simulation;

c) average values and standard errors of the H-bond angle in MD simulation

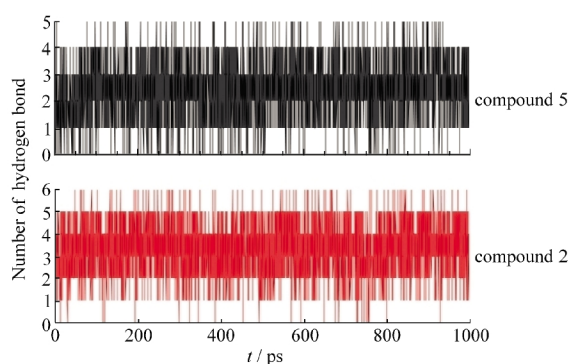


Fig.5 Number of hydrogen bonds formed between R2 group of inhibitors and the active site of PTP1B during the 1 ns MD simulations

could be explained by an unconventional hydrogen bond between fluorine atom and Phe182 of PTP1B. According to our study and the Burke's investigation, the fluorine atom as a hydrogen bond donor is helpful to improve the electronic interaction of inhibitor with the active site of PTP1B.

3 Conclusions

The binding models between five DFMP or DFMS inhibitors and PTP1B were proposed by using molecular docking. The CF₂-phosphonate/sulfonate groups binding to the primary active site and the sulfuryamide groups are located in the secondary active site. Comparing the binding free energies, we find that the difference of binding between the non-peptide DFMP and DFMS inhibitors are directly related to residue Arg221 in the primary active site of PTP1B. The electrostatic interactions between inhibitor and Arg221 are extremely important for the binding preference of the DFMP inhibitors, and the van der Waals interactions are extremely important for the binding preference of the DFMS inhibitors. Compounds with more negative charge have better binding affinity than those with less negative charge, but the electron withdrawing group or atom, such as fluorine, locate on α carbon of phosphonate/sulfonate groups may reduce the binding affinity.

A stable hydrogen bond was found between the fluorine atom of the CF₂-phosphonate/sulfonate groups and Arg221 of PTP1B, so hydrogen bond donor atoms with appropriate radii will be helpful to improve the electronic interaction of inhibitor with the active site of PTP1B, especially for those dianionically groups. All above simulation results are in good agreement with the experimental data and provide us helpful information for structured-based design of PTP1B phosphotyrosine mimetics inhibitors.

Acknowledgments: We thank Prof. Xiaojie Xu in College of Chemistry and Molecular Engineering of Peking University for providing access to computer software such as AMBER. We are grateful to Prof. Scott Taylor in the Department of Chemistry, University of Waterloo, Canada, who shared the bioactivity and synthesis data with us.

References

- Hunter, T. *Cell*, **1995**, *80*(2): 225
- Alonso, A.; Sasin, J.; Bottini, N.; Friedberg, I.; Osterman, A.; Godzik, A.; Hunter, T.; Dixon, J.; Mustelin, T. *Cell*, **2004**, *117*(6): 699
- Elchebly, M.; Payette, P.; Michaliszyn, E.; Cromlish, W.; Collins, S.; Loy, A. L.; Normandin, D.; Cheng, A.; Himms-Hagen, J.; Chan, C. C.; Ramachandran, C.; Gresser, M. J.; Tremblay, M. L.; Kennedy, B. P. *Science*, **1999**, *283*(5407): 1544
- Zhang, Z. Y. *Curr. Opin. Chem. Biol.*, **2001**, *5*(4): 416
- Rye, C. S.; Baell, J. B. *Curr. Med. Chem.*, **2005**, *12*(26): 3127
- Burke, T. R.; Yao, Z. J.; Liu, D. G.; Voigt, J.; Gao, Y. *Biopolymers*, **2001**, *60*(1): 32
- Burke, T. R.; Kole, H. K.; Roller, P. P. *Biochem. Biophys. Res. Commun.*, **1994**, *204*(1): 129
- Yao, Z. J.; Ye, B.; Wu, X. W.; Wang, S.; Wu, L.; Zhang, Z. Y.; Burke, T. R. *Bioorg. Med. Chem.*, **1998**, *6*(10): 799
- Taylor, S. D.; Kotoris, C. C.; Dinaut, A. N.; Wang, Q.; Ramachandran, C.; Huang, Z. *Bioorg. Med. Chem.*, **1998**, *6*(9): 1457
- Shen, K.; Keng, Y. F.; Wu, L.; Guo, X. L.; Lawrence, D. S.; Zhang, Z. Y. *J. Biol. Chem.*, **2001**, *276*(50): 47311
- Dufresne, C.; Roy, P.; Wang, Z.; Asante-Appiah, E.; Cromlish, W.; Boie, Y.; Forghani, F.; Desmarais, S.; Wang, Q.; Skorey, K.; Waddleton, D.; Ramachandran, C.; Kennedy, B. P.; Xu, L.; Gordon, R.; Chan, C. C.; Leblanc, Y. *Bioorg. Med. Chem. Lett.*, **2004**, *14*(4): 1039
- Lau, C. K.; Baylym, C. I.; Gauthier, J. Y.; Li, C. S.; Therien, M.; Asante-Appiah, E.; Cromlish, W.; Boie, Y.; Forghani, F.; Desmarais, S.; Wang, Q.; Skorey, K.; Waddleton, D.; Payette, P.; Ramachandran, C.; Kennedy, B. P.; Scapin, G. *Bioorg. Med. Chem. Lett.*, **2004**, *14*(4): 1043
- Barford, D.; Flint, A. J.; Tonks, N. K. *Science*, **1994**, *263*(5152): 1397
- Leung, C.; Grzyb, J.; Lee, J.; Meyer, N.; Hum, G.; Jia, C.; Liu, S.; Taylor, S. D. *Bioorg. Med. Chem.*, **2002**, *10*(7): 2309
- Hussain, M.; Ahmed, V.; Hill, B.; Ahmed, Z.; Taylor, S. D. *Bioorg. Med. Chem.*, **2008**, *16*(7): 6764
- Hou, T. J.; Chen, K.; McLaughlin, W. A.; Lu, B. Z.; Wang, W. *Plos. Comput. Biol.*, **2006**, *2*(1): 46
- Hou, T. J.; Guo, S. L.; Xu, X. J. *J. Phys. Chem. B*, **2002**, *106*(21): 5527
- Hou, T. J.; Yu, R. *J. Med. Chem.*, **2007**, *50*(6): 1177
- Hou, T. J.; Zhu, L. L.; Chen, L. R.; Xu, X. J. *J. Chem. Inf. Comput. Sci.*, **2003**, *43*(1): 273
- Lee, M. R.; Duan, Y.; Kollman, P. A. *Proteins-Structure Function and Genetics*, **2000**, *39*(4): 309
- Huo, S. H.; Wang, J. M.; Cieplak, P.; Kollman, P. A.; Kuntz, I. D. *J. Med. Chem.*, **2002**, *45*(7): 1412
- Wang, J. M.; Morin, P.; Wang, W.; Kollman, P. A. *J. Am. Chem. Soc.*, **2001**, *123*(22): 5221

- 23 Berman, H. M.; Westbrook, J.; Feng, Z.; Gilliland, G.; Bhat, T. N.; Weissig, H.; Ilya, N.; Shindyalov, I. N.; Bourne, P. E. *Nucleic Acids Res.*, **2000**, **28**(1): 235
- 24 SYBYL molecular simulation package. <http://www.sybyl.com>, 2004
- 25 Frisch, M. J.; Trucks, G. W.; Schlegel, H. B.; *et al.* Gaussian 03, Revision B.01. Pittsburgh, PA: Gaussian Inc., 2003
- 26 Bayly, C. I.; Cieplak, P.; Cornell, W. D.; Kollman, P. A. *J. Phys. Chem.*, **1993**, **97**(40): 10269
- 27 Case, D. A.; Cheatham, T. E.; Darden, T.; Gohlke, H.; Luo, R.; Merz, K. M.; Onufriev, A.; Simmerling, C.; Wang, B.; Woods, R. J. *J. Comput. Chem.*, **2005**, **26**(16): 1668
- 28 Morris, G. M.; Goodsell, D. S.; Halliday, R. S.; Huey, R.; Hart, W. E.; Belew, R. K.; Olson, A. J. *J. Comput. Chem.*, **1998**, **19**(14): 1639
- 29 Duan, Y.; Wu, C.; Chowdhury, S.; Lee, M. C.; Xiong, G.; Zhang, W.; Yang, R.; Cieplak, P.; Luo, R.; Lee, T.; Caldwell, J.; Wang, J.; Kollman, P. *J. Comput. Chem.*, **2003**, **24**(16): 1999
- 30 Wang, J. M.; Wolf, R. M.; Caldwell, J. W.; Kollman, P. A.; Case, D. A. *J. Comput. Chem.*, **2004**, **25**(9): 1157
- 31 Jorgensen, W. L.; Chandrasekhar, J.; Madura, J. D.; Impey, R. W.; Klein, M. L. *J. Chem. Phys.*, **1983**, **79**(2): 926
- 32 Morishita, T. *J. Chem. Phys.*, **2000**, **113**(8): 2976
- 33 Ryckaert, J. P.; Ciccotti, G.; Berendsen, H. J. C. *J. Comput. Phys.*, **1977**, **23**(3): 327
- 34 Darden, T.; York, D.; Pedersen, L. *J. Chem. Phys.*, **1993**, **98**(12): 10089
- 35 Kollman, P. A.; Massova, I.; Reyes, C.; Kuhn, B.; Huo, S.; Chong, L.; Lee, M.; Lee, T.; Duan, Y.; Wang, W.; Donini, O.; Cieplak, P.; Srinivasan, J.; Case, D. A.; Cheatham, T. E. *Acc. Chem. Res.*, **2000**, **33**(12): 889
- 36 Wang, J. M.; Hou, T. J.; Xu, X. *J. Curr. Comput. -Aided Drug Des.*, **2006**, **2**(20): 287
- 37 Tsui, V.; Case, D. A. *J. Am. Chem. Soc.*, **2000**, **122**(11): 2489
- 38 Gohlke, H.; Kiel, C.; Case, D. A. *J. Mol. Biol.*, **2003**, **330**(4): 891
- 39 Hou, T. J.; Zhang, W.; Case, D. A.; Wang, W. *J. Mol. Biol.*, **2008**, **376**(4): 1201
- 40 Wallace, A. C.; Laskowski, R. A.; Thornton, J. M. *Protein Eng.*, **1995**, **8**(2): 127
- 41 Burke, T. R.; Ye, B.; Yan, X. J.; Wang, S. M.; Jia, Z. C.; Chen, L.; Zhang, Z. Y.; Barford, D. *Biochemistry*, **1996**, **35**(50): 15989